Appearance-potential study of the 4f states of holmium

D. Chopra, H. Babb, and R. Bhalla

Physics Department, East Texas State University, Commerce, Texas 75428
(Received 1 July 1976)

The soft-x-ray appearance-potential spectra (SXAPS) of $M_{4,5}$ and $N_{4,5}$ levels of rare-earth metal holmium (^{165}Ho) have been obtained in the 130–1400-eV range with a simple, nondispersive spectrometer which measures the derivative of the total x-ray fluorescence of the anode surface as a function of bombarding electron energy. The spectrum represents the differential excitation probability of $3d$ and $4d$ core levels and mirrors the self-convolution of the density of empty $4f$ states in Ho. The M_5 peak shows two distinct components, 1.8 eV apart, followed by two satellites at 5.7 and 8.7 eV and a secondary peak at 33.5 eV above the M_5 threshold. The $N_{4,5}$ spectrum is more complex, consisting of two prominent peaks. The more intense peak appears at 10.2 eV above the $N_{4,5}$ threshold in agreement with theoretical calculations. The spectral features have been discussed in terms of the existing excitation state and satellite line theories. The binding energies of the M_4, M_5, and $N_{4,5}$ levels of Ho were, however, found to be consistently a few eV lower than those found by most other techniques.

INTRODUCTION

Soft-x-ray appearance-potential spectroscopy (SXAPS) has been recognized as a technique for studying the surface properties of solids. These include element identification, chemical shift determination, and investigation of the electronic states of atoms at solid surfaces. A monochromatic electron beam striking the solid surface excites a soft-x-ray flux consisting of bremsstrahlung and characteristic radiation. The yield of this fluorescence process increases abruptly at the threshold energies for core-level excitation and this increase is proportional to the probability of excitation. In the simple one-electron picture, this probability will be determined by the densities of initial and final electronic states. The onset of SXAPS peaks, therefore, corresponds to the binding energy at which the core electrons can be excited to unoccupied states. The subsidiary structure beyond the threshold is expected to reveal information regarding the density of unfilled valence states above the Fermi level. Unfortunately, bremsstrahlung and low-energy characteristic processes tend to obscure the characteristic x-ray lines. The first attempts to extract the onset of characteristic radiation by graphical differentiation of the excitation curve were made in the early 1900's.[1-3] Renewed interest in SXAPS commenced with the development of potential modulation differentiation and ultrahigh-vacuum techniques.[4,5] SXAPS was developed into its present form by Park, Houston, and Schreiner[6] in 1970. Several recent review articles[7-10] have summarized the experimental results and various theories of SXAPS.

The present paper describes the application of soft-x-ray appearance-potential technique to rare-earth elements. Theories of soft-x-ray absorption and emission in metals predict that the $M_{4,5}$ and $N_{4,5}$ edges in rare-earth metals will be particularly well enhanced and, therefore, quite suitable for study by the appearance-potential technique. The importance of rare-earth metals to modern technology has stimulated experimental studies of their electronic structure. The position of the $4f$ states relative to the Fermi energy in rare-earth metals is important for understanding their unique magnetic, electrical, and optical properties. SXAPS measurements on some actinides and lanthanides have been reported previously.[11-14] The purpose of this paper is to report the SXAPS studies on holmium (Ho).

EXPERIMENT

The spectrometer used in the present investigation is shown schematically in Fig. 1. The spectrometer chamber is constructed of 304 stainless steel using metal gaskets to minimize outgasing. The system operating pressure was kept below 10^{-8} Torr for measurements reported here by a triode VacIon pump. The addition of an encasing oven that allows baking of the chamber walls and the pump at temperatures of 200–250 °C reduced the pressure to 10^{-9} Torr range. The bakeout is highly desirable for extended low-pressure operation. The necessity of ultrahigh vacuum is evident in the consideration that a monolayer of contaminants forms on the target in less than two hours at a vacuum less than 10^{-10} Torr.[7] Inside the chamber the target and filament are mounted on high-vacuum feed through flange. The filament is a fine tungsten wire mounted close to the target for stable operation of the spectrometer at low accelerating potentials. The detector assembly is

FIG. 1. Simplified schematic diagram of the soft-x-ray appearance-potential spectrometer. The grid is biased -50 V relative to the filament to prevent the filament emission from reaching the detector assembly. The filament is heated by an 8% duty cycle 20-V 400-Hz pulse to improve the resolution and signal-to-noise ratio. The potential of the target is modulated by the isolation transformer and swept by the programmable dc power supply. The component of the detector current corresponding to the potential oscillation on the target is selected by a tuned circuit and phase-lock amplifier.

mounted on another flange on the opposite end of the chamber and is screened from the filament-target assembly by a nickel wire mesh grid. This grid is biased at −50 V relative to the filament. The function of the grid is to prevent the thermal electrons from reaching the detector assembly. The detector consists of two intersecting nickel planes biased at + 300 V mounted normal to the target. The chamber walls act as a photocathode.

Electrons from the filament are accelerated to produce soft x rays upon impinging on the target. The filament is operated by an emission control unit which maintains a constant emission current irrespective of the target potential. The potential on the target is varied from 0 to 2000 V by a variable slope ramp generator. The same potential drives the abscissa of the x-y recorder. In order to record the spectrum, the target potential is linearly varied through the desired voltage range. The resulting x rays pass through the grid and strike the chamber wall, generating photoelec-

trons. These electrons are collected by the detector. As the target potential approaches threshold for core-level excitation of surface atoms, the x-ray production increases abruptly with energy. Extraction of the signal from the background is accomplished by differentiation of the signal. This is accomplished by superimposing a 0.5-V_{p-p} 4.5-kHz excitation signal on the accelerating voltage. This excitation voltage causes the x-ray intensity, I, to vary at a 4.5 kHz rate, the amplitude and phase of the variation being proportional to $\Delta I/\Delta V$ of the intensity curve between $V+0.25$ V and $V-0.25$ V, where V is the accelerating voltage. Detection is accomplished by filtering the photoelectron current to extract the 4.5-kHz component which is then amplified and synchronously rectified to provide a dc level corresponding to the slope of the x-ray intensity. This signal drives the ordinate of a x-y recorder. The appearance-potential spectrum is plotted in terms of the detector output versus the accelerating potential. The emission current, modulation voltage, and time constant of the phase-lock amplifier were adjusted to record the precise spectra as determined by the signal-to-noise ratio and peak width at half-maximum. No soft-x-ray filter in the form of Al foil or Mylar was used to reduce the shot noise and ac coherent noise.

The resolution of the spectrometer is dependent upon the stability of the target potential, the modulation potential and the voltage drop across the filament. The modulation voltage held at approximately 0.5 V peak-to-peak works adequately. Monoenergetic bombarding electrons were produced by eliminating voltage drop across the filament. This was accomplished by operating the spectrometer in a filament-off detector-on mode.[15] This chopped, filament heating current and gated counter technique resulted in the ability to bombard the target with electrons whose effective spread in energy in less than about 0.2 eV. An alternate technique of heating the filament by an 8% duty cycle 20-V 400-Hz pulse not only resulted in a similar reduction in the energy spread of bombarding electrons but also improved the signal-to-noise ratio by a factor of 2. The total width of the spectral window of the instrument, determined by comparison of published L spectra of titanium with that recorded in this work, was estimated to be less than 1.5 eV.

High-purity Ho in the form of polycrystalline $1 \times \frac{1}{2} \times \frac{1}{30}$ in.[3] was obtained from Alfa Inorganic Inc. The target was cleaned by argon sputtering and annealed at a 2000-V 10-mA x-ray tube setting for about an hour. The entire process of cleaning the target and scanning the spectrum over a range of 100 V can easily be accomplished in less than

2 h. Since the samples used were not prepared *in situ*, the possibilities of impurity migration from the bulk, contamination with any residual gas, and a change of target structure due to argon bombardment are present.

RESULTS

Holmium has an electronic configuration of $5p^6 4f^{11} 6s^2$. The $M_{4,5}$ appearance-potential spectra of Ho (Fig. 2) was recorded at an emission current of 2 mA. The M_5 spectrum shows a narrow intense peak and an undershoot. Considering the narrowness of the structure, it is logical to assign this peak to the $M_5 - N_{6,7}$ transition. The difference between the maxima of the positive peak and the undershoot reflects the degree of mixing of the empty states of different symmetry at the Fermi level. The M_5 peak consists of two distinct components approximately 1.8 eV apart and exhibits a pronounced shoulder on the low-energy side. There is also evidence of two satellites on the high-energy side of the M_5 peak as can be seen by inspection of Fig. 2. These satellites are relatively weak but were consistently recorded at approximately 5.7 and 8.7 eV from the M_5 threshold. Another secondary broad peak shows up at approximately 33.5 eV above the M_5 threshold. The smaller peak and almost negligible undershooting in the case of M_4 spectrum implies a decrease in probability of M_4-$N_{6,7}$ transition. Following the M_4 and the M_5 peaks the trace dips below the base line, indicating an enhanced transition probability at the threshold. A highly simplified representa-

tion of SXAPS approximates the width of the empty $4f$ band by the width of the positive peak. This width measured at half-maximum and corrected for instrumental distortion has been found to be 2.6 eV. The N spectra shown in Fig. 3 exhibits several additional peaks associated with the $N_{4,5}$ level of Ho. Two main peaks are resolved and clearly identifiable as separate peaks. The relatively intense peak seems to split into a doublet structure as indicated by a dip in the signal strength. The remaining peaks are relatively narrow and neither intense nor symmetric, and give the appearance of superposition on the broad band. The base width of this band has been determined to be approximately 20 eV. The spectrum is representative of many runs. Near the threshold the spectrum should roughly reflect the density of unoccupied states.[16] For metals the binding energy should correspond to the Fermi level represented by the abrupt discontinuity in the density of empty states. Thus the point of intersection of the extrapolated base line and low-energy edge of the peak determines the Fermi energy. The threshold energies of the peaks were corrected for the work function of the tungsten emitter, the modulation of the sample potential, and the thermal energy spread of the bombarding electrons. In the present measurements the total correction amounted to approximately 5.0 eV. The binding energies determined in this way are given in Table I and compared to values obtained by other methods. Table II lists the positions of the additional peaks and their relative energy difference from the threshold energies of the peaks allowed by normal dipole selection rules.
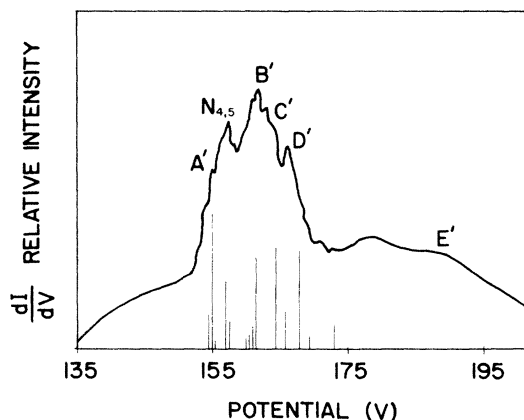

FIG. 2. Holmium M_4 and M_5 soft-x-ray appearance potential spectrum. Electron current 2 mA, modulation potential 0.5 V_{p-p}. The derivative of the photocurrent (I) with respect to electron accelerating potential (V) is plotted vs V.

FIG. 3. Holmium $N_{4,5}$ soft-x-ray appearance potential spectrum from 135 to 195 eV (electron current 1 mA, modulation potential 0.5 V_{p-p}) is compared with calculated photoabsorption spectrum from Ref. 26.

TABLE I. Electronic binding energies of holmium (eV).

Peak	SXAPS[a]	Bearden and Burr[b]	Fischer and Baun[c]	Lotz[d]
M_4	1387.3 ± 0.4	1391.5 ± 0.7	1384.3	1395
M_5	1347.5 ± 0.4	1351.4 ± 0.8	1343.7	1354
$N_{4,5}$	158.0 ± 0.5	161.0 ± 1.0	$\cdots$	172
				164

[a] The SXAPS are experimental values derived from present measurements.

[b] Reference 17.

[c] Reference 23.

[d] The electron binding energies (ionization energies) of all subshells are calculated for free atoms by W. Lotz, J. Opt. Soc. Am. 60, 206 (1970).

DISCUSSION

As can be seen from Table I, the M_4 and M_5 energy levels of Ho surface atoms determined in this work are lower than the bulk atoms as reported by Bearden and Burr.[17] The agreement between the present $N_{4,5}$ values and those of Bearden and Burr is within 3 eV. The discrepancy is partially due to the lowering of the interatomic effects at the surface of the target, the difficulty of determining the thresholds of peaks due to a decrease in signal-to-noise ratio, the auger lifetime broadening of the core levels, and the instrument distortion.

The holmium target also exhibited a weak oxygen K peak at 532 eV. The reactivity of Ho with oxygen at pressures of 10^{-9} Torr implies that the sample was partially Ho oxide. The impurities are expected to have some influence upon the results reported here. Previous measurements on rare-earth elements by Murthy and Redhead,[14] and Park and Houston[11] show minimal changes in spectral features on oxidation. Consequently, oxidation of holmium is not expected to result in significant changes in the spectra. Shifts in core-level binding energies due to oxidation in actinide uranium were less than 0.2 eV.[11] The resonant line phenomenon reported in some lanthanides[13] was clearly observable as a multiplet structure in the M_5 peak.

TABLE II. Peak positions in holmium above the threshold (eV).

M_5 threshold	$\cdots$	$N_{4,5}$ threshold	$\cdots$
M_5	2.4	A'	3.3
B	4.2	$N_{4,5}$	5.5
C	5.7	B'	10.2
D	8.7	C'	11.6
E	33.5	D'	14.2
M_4 threshold	$\cdots$		
M_4	3.4		

Chamberlain and Baun[13] have observed a similar representation of line isochromat in the M_5 spectra of Sm and attribute the low-energy component (designated as M_5 in Fig. 2) to the x-ray yield from the principal M_5 x-ray line. According to their interpretation, the incident electron and $3d_{5/2}$ (or $4d_{5/2}$) electron are excited to double occupancy of a normally empty bound-ejected-electron state of $4f$ symmetry. The high-energy resonant line (B) results from the transition of one of the bound electrons to fill a $3d$ (or $4d$) core hole. The other electron ascends to an available state in the conduction band. The bound-ejected-electron state couples the fast electron-atom system to the slow electron-x-ray-atom system and generates energy-dependent resonances in the inelastic electron scattering cross section. The effect is thought to depend upon the large overlap of $3d$ or $4d$ states with conduction band states of $4f$ symmetry and is predicted for M_5 and N_5 lines in most lanthanides, M_4 and N_4 levels in light lanthanides and $M_5, M_4, N_5, N_4, O_5, O_4$ levels of light actinides. These linelike resonances have also been observed in the M_α, M_β emission spectra of light rare earths (La, $Z = 57$, and Ce, $Z = 58$) excited with electrons of energy near the ionization threshold of M_5 and M_4 levels, respectively.[18]

Laramore[19] has extended the model used by Nozières and De Dominicis[20] for calculating the threshold behavior of x-ray emission and absorption in metals to the SXAPS where a core-level excitation is caused by a fast electron. This theory predicts divergent threshold behavior accompanying the s-state core-level transition for SXAPS. Wertheim et al.[21] explain the satellite peaks on the basis of excitation from valence band to unoccupied $4f$ levels. The absence of satellites following the M_1, M_2, and M_3 peaks of La and Gd is contrary to this explanation.[14] Chang and Langreth[22] have considered the interaction of slow electrons with plasmons by perturbation theory and predict the association of strong plasmon satellites with slow-slow coupling in SXAPS.

The present investigation measures the separation of the two peaks of M_5 series characteristic x-ray line from M_4 peak as 40.8 ± 0.5 and 39.0 ± 0.5 eV, respectively. The energy difference between the Ho M_5 and M_4 x-ray absorption-edge positions was determined by Fischer and Baun[23] to be 40.6 eV. Bearden and Burr[17] report the corresponding spin-doublet splitting to be 40.1 eV. The apparent agreement of these values with the observed energy difference of lower-energy M_5 component from M_4 peak suggests that the origin of the lower-energy peak of M_5 SXAPS in Fig. 2 is directly related to the onset of the M_5 series x-ray line. The other peak, B, is believed to result from the quasi-

monochromatic x-ray emission line which arises from the scattering of the incident electron into an f state of the excited atom. This singularity appears to follow the dipole selection rule. The M_4 peak does not seem to depict any significant multiple structure components.

Satellites similar to those observed at approximately 5.7 and 8.7 eV from the threshold have been reported for La and Gd.[14] Since the linelike x-ray emission accompanying the near threshold excitation of M_5 level is believed to be a single quasi-monochromatic line instead of a series of lines, the explanation of these satellites must be sought somewhere else. These satellites may result from plasmon energy losses as a result of coupling between the collective modes of conduction electrons and the core hole. Such satellites have been reported in the SXAPS of boron, graphite, and oxygen.[24] The surface plasmon energy of rare-earth metals neighboring Ho is approximately 7 eV which corresponds to the position of the first satellite. The second satellite observed at approximately 8.7 eV may then be associated with the bulk-plasmon energy loss which is predicted to be 11 eV. The broad peak located at 33.5 eV from the M_5 threshold may be attributed to the plasmon energy loss of higher order. It will be interesting to compare these results with soft-x-ray absorption spectra (SXA). The $M_{4,5}$ x-ray absorption spectrum of Ho recorded by Fischer and Baun,[23] which exhibits four peaks associated with M_5 edge and single peak for M_4 edge, agrees with this study. Since selection rules are not rigidly obeyed in SXAPS, as in the case of photoexcitation,[16] SXA of all symmetries must be considered for correlating spectral features in SXAPS and SXA.

The $N_{4,5}$ SXAPS exhibits two main peaks located at approximately 5.5 and 10.2 eV above the $N_{4,5}$ threshold. The more intense peak, which possesses considerable secondary structure, evidently splits into two components. The onset of the x-ray yield is observed at 158.0 eV. Numerous weak lines also appear near the threshold as on the broad band. These lines were consistently reproduced and are likely to represent the transitions involving the core level and excitation states. In addition to the above features a broad peak was observed at approximately 37 eV for the $N_{4,5}$ threshold. This peak appears as an entity separate from the broad band.

Dehmer et al.[25] have attributed the broad peaks in the photoabsorption spectra of rare-earth metals above the $4d$ edge to $4d^{10}4f^N \rightarrow 4d^94f^{N+1}$ transitions. According to their interpretation, a centrifugal potential barrier of 10–20 eV prevents low-energy f orbits from overlapping the $4d$ orbits for $Z < 57$.

However for $Z \geq 57$, $4f$ orbits contract and admix with $4d$ orbits. The $5f$ and higher discrete orbits and low-energy f continuum remain suppressed by the barrier. Accordingly $4d$–$4f$ photoabsorption spectrum involves transitions from ground level of a $4d^{10}4f^N$ configuration to numerous levels of a $4d^94f^{N+1}$ configuration which extend over a broad range of ≥ 20 eV as a result of exchange interaction between the f electrons and d vacancy. This interaction is stronger between subshells with the same principal quantum number. Sugar[26] has calculated the energy levels and their weighted oscillator strengths for Ho^{+3} $4d^{10}f^{10}$–$4d^94f^{11}$ transitions.

Figure 3 shows a comparison of present $N_{4,5}$ SXAPS of Ho with calculated positions and relative oscillator strengths. The vertical lines represent the calculated spectrum with relative peak values determined by the oscillator strength scale. Some peaks result from a blend of two or more lines. It is believed that strong absorption peaks usually arise from transitions involving high-purity levels. We have attempted to identify the observed main peaks with the few calculated strong lines. The overall accuracy of the predicted positions varies from 0.2 to 0.5 eV. The comparison is not considered strictly valid since SXAPS corresponds to the transition of two electrons into the conduction band in contrast with SXA where a single electron is involved. Furthermore, in the case of rare-earth metals with a more than half-filled $4f$ shell, the oscillator strength is divided between the ^3H and ^3G terms in the ratio of 1:3. According to Sugar,[26] these terms depend on ^1G and are separated by 10 eV, predicting the interval between the onset of absorption and the more intense peak to be on the order of 10 eV. The interval of the present $N_{4,5}$ SXAPS is measured as 10.2 and the base width as 20 eV. Both measurements are in good agreement with the calculations of the $4d^94f^{N+1}$ energy levels and relative oscillator strengths of the transitions involved in Ho.

Sugar has also invoked the overlap of $4f$ and $3d$ orbits to account for the observed line structure in the vicinity of the M_4 and M_5 photoabsorption edges of La, Er, and Tm. The overlap in this case is much less than that of $4f$ with $4d$. Consequently, the spin-orbit interval is preserved and relatively few lines are predicted near the positions of M_4 and M_5 edges. These lines result from $3d^{10}4f^N \rightarrow 3d^94f^{N+1}$ transitions. His calculated M_4 and M_5 photoabsorption spectra are in good agreement with the experimental results.[27,28] Er and Ho, being neighboring elements of the lanthanide family, are expected to follow the same general trend. To correlate their characteristics further computation of the eigenvalues of the ex-

citation states of $3d^9 4f^{12}$ and $4d^9 4f^{12}$ configurations in Ho are needed. These calculations are expected to provide a plausible interpretation of the spectra reported in this paper.

CONCLUSION

It is evident from the foregoing that the Ho $M_{4,5}$ and $N_{4,5}$ SXAPS do not follow the simple one electron theory. We have compared the SXAPS with photoabsorption spectra and have attempted to explain some of the observed spectral features by quantitative arguments using simplifying assumptions. Because the incident electrons are at threshold excitation energies, SXAPS samples a shallow layer of the solid and provides information characteristic of the surface atoms. The binding energies of M_4, M_5, and $N_{4,5}$ levels of Ho were determined to be consistently a few eV lower than those based on other techniques. The differences are in excess of the uncertainties in the determination of absolute binding energies. The discrepancies directly result from reduced coordination of Ho surface atoms in accordance with the measurements of Houston et al.[29] on $3d$ transition metals and of Redhead and Richardson[12] on thorium. The shifts in core-level binding energies as a re-

sult of some oxidation of holmium surface are not expected to be more than 0.2 eV.

The presence of two distinct peaks in the spectra of M_5 and $N_{4,5}$ levels imply a double peaked density of $4f$ states in holmium. This feature is also interpreted as a singularity in the x-ray yield when the electron-excitation energy is near the ionization potential of either the M_5 or N_5 level. Additional spectral features associated with the M_5 and $N_{4,5}$ peaks seem to complicate this explanation. The origin of the spectral features must be understood before any meaningful measurement of spectral parameters are made. The preliminary calculations of the energy levels of $4d^9 4f^{11}$ configuration in Ho are found to be in general accord with the experiment. A more detailed and precise theory of the excitation of SXAPS of rare-earth metals is likely to provide a more plausible explanation of spectral features of holmium reported in this work. Additional experimental data on the spectra of other rare earths should help in the development and testing of the proposed theoretical calculations.

ACKNOWLEDGMENTS

[1]W. H. B. Skinner, Proc. R. Soc. Lond. A 135, 84 (1932).

[2]J. Franck and G. Hertz, Verh. Dtsch. Phys. Ges. 16, 12 (1911).

[3]O. W. Richardson and C. B. Bazzoni, Philos. Mag. 42, 1015 (1921).

[4]G. Shinoda, T. Suzuki, and S. Kato, J. Phys. Soc. Jpn. 7, 644 (1952).

[5]P. A. Redhead, Bull. Radio Electr. Eng. Div. Nat. Res. Counc. Can. 16, 41 (1966).

[6]R. L. Park, J. E. Houston, and D. G. Schreiner, Rev. Sci. Instrum. 41, 1810 (1970).

[7]R. L. Park and J. E. Houston, J. Vac. Sci. Technol. 11, 1 (1974).

[8]A. M. Bradshaw, Surf. Defect Prop. Solids 3, 153 (1973).

[9]J. C. Tracy, J. Appl. Phys. 43, 4164 (1972).

[10]R. L. Park, Surf. Sci. 48, 80 (1975).

[11]R. L. Park and J. E. Houston, Phys. Rev. A 7, 1447 (1973).

[12]P. A. Redhead and G. W. Richardson, J. Appl. Phys. 43, 2970 (1972).

[13]M. B. Chamberlain and W. L. Baun, J. Vac. Sci. Technol. 11, 441 (1974).

[14]M. S. Murthy and P. A. Redhead, J. Vac. Sci. Technol. 11, 837 (1974).

[15]L. H. Germer, Phys. Rev. 25, 795 (1925).

[16]P. O. Nilsson and J. Kanski, Surf. Sci. 37, 700 (1973).

[17]J. A. Bearden and A. F. Burr, Rev. Mod. Phys. 39, 125 (1967).

[18]M. B. Chamberlain, Ph.D. thesis (New Mexico State University, 1970) (unpublished).

[19]G. E. Laramore, Phys. Rev. Lett. 27, 1050 (1971).

[20]P. Nozières, and C. T. De Dominicis, Phys. Rev. 178, 1097 (1969).

[21]G. K. Wertheim, R. L. Cohen, A. Rosencwaig, and H. J. Guggenheim, in Electron Spectroscopy, edited by D. A. Shirley (North-Holland, Amsterdam, 1972).

[22]Jhy-Jiun Chang and David C. Langreth, Phys. Rev. B 5, 3512 (1972).

[23]David W. Fischer and William L. Baun, J. Appl. Phys. 38, 4830 (1967).

[24]J. E. Houston and Robert L. Park, J. Chem. Phys. 55, 4601 (1971); J. Vac. Sci. Technol. 8, 91 (1971).

[25]J. L. Dehmer, A. F. Starace, U. Fano, J. Sugar, and J. W. Cooper, Phys. Rev. Lett. 26, 1521 (1971).

[26]Jack Sugar, Phys. Rev. B 5, 1785 (1972); Phys. Rev. A 6, 1764 (1972).

[27]E. A. Stewardson and J. E. Wilson, Proc. Phys. Soc. Lond. A 69, 93 (1956).

[28]K. C. Williams, Proc. Phys. Soc. Lond. 87, 983 (1966).

[29]J. E. Houston, R. L. Park, and G. E. Laramore, Phys. Rev. Lett. 30, 846 (1973).